

LETTERS

In vivo imaging of haematopoietic cells emerging from the mouse aortic endothelium

Jean-Charles Boisset^{1,2}, Wiggert van Cappellen³, Charlotte Andrieu-Soler¹, Niels Galjart¹, Elaine Dzierzak^{1,2} & Catherine Robin^{1,2}

Haematopoietic stem cells (HSCs), responsible for blood production in the adult mouse, are first detected in the dorsal aorta starting at embryonic day 10.5 (E10.5)^{1–3}. Immunohistological analysis of fixed embryo sections has revealed the presence of haematopoietic cell clusters attached to the aortic endothelium where HSCs might localize^{4–6}. The origin of HSCs has long been controversial and several candidates of the direct HSC precursors have been proposed (for review see ref. 7), including a specialized endothelial cell population with a haemogenic potential. Such cells have been described both *in vitro* in the embryonic stem cell (ESC) culture system^{8,9} and retrospectively *in vivo* by endothelial lineage tracing^{5,10} and conditional deletion experiments¹¹. Whether the transition from haemogenic endothelium to HSC actually occurs in the mouse embryonic aorta is still unclear and requires direct and real-time *in vivo* observation. To address this issue we used time-lapse confocal imaging and a new dissection procedure to visualize the deeply located aorta. Here we show the dynamic *de novo* emergence of phenotypically defined HSCs (*Sca1*⁺, *c-kit*⁺, *CD41*⁺) directly from ventral aortic haemogenic endothelial cells.

Live imaging technology and confocal microscopy are powerful tools to observe the development of cells in real-time and in their native and intact environment. The transparency of zebrafish embryos has allowed the rapid advancement of studies showing the dynamic development of the haematopoietic system^{12,13}. Live studies in mouse embryos have thus far been hampered because the aorta is located deep within the opaque embryo. To address the question of whether HSCs are derived from aortic haemogenic endothelial cells in the mouse embryo, we developed a new experimental approach to access and visualize live cells in the dynamic and physiological context of the aorta. For the experiments, non-fixed mouse embryos (E9 to E11) were cut into thick transverse sections (Fig. 1a–c). Using this strategy the architecture and organization of the aorta and surrounding tissues were conserved (Fig. 1b, c). The intra-aortic blood was flushed away and fluorochrome-conjugated antibodies specific for haematopoietic and endothelial cell surface proteins were either injected into the aorta before embryo sectioning (Fig. 1a, protocol a), or incubated with the slices after embryo cutting (Fig. 1a, protocol b). Embryo slices were subsequently imaged under the confocal microscope. Both staining protocols gave similar patterns of surface marker expression on cells located in the aorta (Supplementary Fig. 1). Transgenic embryos (*Ly-6A-GFP*) expressing GFP (green fluorescent protein) under the control of the *Ly-6A* (also known as *Ly6a* or *Sca1*) transcriptional elements were used as it was shown previously that all embryonic and adult HSCs are GFP⁺ (ref. 14). GFP⁺ cells localize to intra-aortic clusters and aortic endothelium, but not to the surrounding mesenchyme as shown on fixed embryo sections¹⁵. The same pattern of expression was observed in the live embryo slices (Fig. 1d, g–k). All aortic endothelial cells and all cells in

the clusters express CD31 (Fig. 1e, g) and CD34 (Fig. 1h). Three-dimensional (3D) representation of the aorta and clusters can be obtained by combining sequential optical sections of an embryo slice (Supplementary Movie 1, Fig. 1e). Multicolour staining (protocol b) allowed a clear visualization of the haematopoietic cells (*Ly-6A-GFP*⁺*c-kit*⁺*CD34*⁺ (Fig. 1h, i) or *Ly-6A-GFP*⁺*CD41*⁺*c-kit*⁺ (Fig. 1j, k) that form the clusters attached to the aortic endothelium (*Ly-6A-GFP*⁺ or GFP[−], *c-kit*[−], *CD41*[−], *CD31*⁺, *CD34*⁺). As a technique validation, E10 *Runx1*^{−/−} embryo slices show no clusters or haematopoietic staining (Supplementary Fig. 2). Thus, our experimental approach provides access to the live aorta for direct cell visualization of fluorescent transgene expression and cell surface markers with antibodies classically used for flow cytometry.

To examine the haemogenic endothelium-HSC transition in the physiological context of the aorta, embryos were isolated at E10.5 (>33 somite pairs (s.p.)), the stage when the first HSCs start to be detected there (as demonstrated by long-term transplantation)³. Although very few HSCs are present at E10.5, the choice of this early time point excludes the possibility that newly generated cells have arisen from proliferation events rather than from *de novo* emergence events. Embryos were stained (intra-aortic) with anti-CD31 antibodies, cut, and live sections were cultured directly under the confocal microscope for sequential time-lapse imaging of up to 15 h (Fig. 1a). Under these conditions cell viability and free cell movement within slices were maintained (see Supplementary Movies). We observed the emergence of very rare round GFP⁺ cells. These cells emerge in the lumen of the aorta, budding directly from ventral CD31⁺GFP⁺ endothelial cells. The ventral cell emergence matches with the ventrally restricted location of HSCs in E11 aorta¹⁶. Two examples of cell emergence are shown in Supplementary Movies 2 and 3. As shown in detail for one example (Fig. 2a and Supplementary Movie 2), the budding process takes approximately 1 h 15 min. Once the cell has rounded up (white arrow), it stays attached to the aortic endothelium.

To improve resolution, embryo slices were imaged at a higher magnification. The better definition of the CD31⁺ endothelium allowed a 3D overview of the aortic lumen and of cell emergence (Fig. 2b–d). One example shows a GFP⁺ cell emerging from the ventral aspect of the aortic tube (Fig. 2c and Supplementary Movie 4, white arrow, front perspective of the aorta). At a slightly later time, another cell also emerges (Fig. 2d and Supplementary Movie 4, yellow arrow, back perspective of the aorta). The emergence takes slightly more than 1 h. The GFP⁺ cells emerge from the endothelial layer and express CD31 after emergence. Images of the z-stack of cell emergence (white arrow in Supplementary Movie 4) were deconvoluted to obtain a better cell definition of the endothelium and of the newly emerged cell (Supplementary Movie 5). From a 3D perspective, a CD31⁺GFP⁺ cell integrated into the aortic endothelial layer appears to divide into two GFP⁺ cells (Fig. 2d and Supplementary Movie 4,

Erasmus Medical Center, ¹Department of Cell Biology, ²Erasmus Stem Cell Institute, ³Department of Reproduction and Development, 3000 CA Rotterdam, The Netherlands.

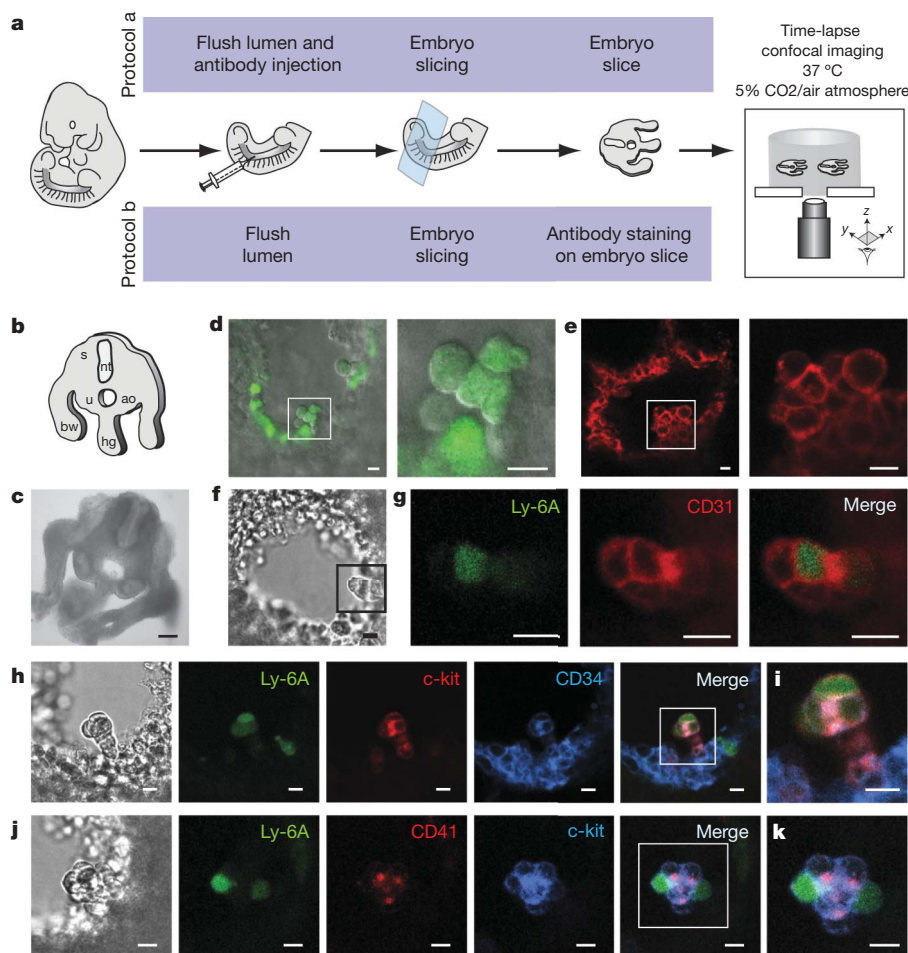


Figure 1 | Visualization of intra-aortic haematopoietic cells by confocal imaging on non-fixed E10 embryo slices. **a**, Protocol scheme. Slices were stained with antibodies before (protocol a) or after (protocol b) embryo slicing and imaged by confocal microscopy. **b**, Schematic of an embryo slice. s, somites; nt, neural tube; u, urogenital ridge; ao, aorta; bw, body wall; hg, hind gut. **c**, Embryo slice. Scale bar, 100 μ m. **d**, *Ly-6A-GFP* embryo slice. Boxed area enlarged in right panel. GFP fluorescent signal is merged with the transmitted light image. **e**, Aortic endothelium and haematopoietic cluster

stained with anti-CD31 antibodies (Protocol a). Boxed area enlarged in right panel (Supplementary Movie 1). **f**, *Ly-6A-GFP* embryo slice (28 to 32 somite pairs, s.p.) stained with Alexa 647-anti-CD31 antibody (red). Black box in **f** (transmitted light) enlarged in **g** (fluorescence). **h-k**, *Ly-6A-GFP* (green) embryo slices (28–32 s.p.) stained with the indicated antibodies directly labelled with phycoerythrin (PE) (red) and allophycocyanin (APC) (blue). White boxes in **h** and **j** are enlarged in **i** and **k** respectively. Scale bars, 10 μ m. Image orientation: ventral side of the embryo downwards.

white arrow). Subsequently, one daughter cell changes position within the endothelium and buds into the aorta lumen (white arrow), whereas the other (asterisk) stays in its original position integrated within the endothelium (Fig. 2d). GFP^+ cell emergence was never observed from the ventral aortic endothelium at E9 (data not shown) or at early E10 ($n = 4$, 27 sections imaged, range from 25 to 32 s.p. stage), times when no HSCs are detected yet. Moreover, no emergence events were observed in *Runx1*^{-/-} embryo slices (data not shown).

All the emerging cells observed express GFP (*Ly-6A-GFP* expression marks all HSCs in the aorta¹⁵). To confirm the haematopoietic identity and immaturity of the emerging GFP^+ cells, embryo slices were stained after overnight culture with antibodies against *c-kit* (also known as Kit), a classical aorta-gonad-mesonephros (AGM) HSC marker¹⁷. An example of a section where an emergent event was observed (Fig. 2e and Supplementary Movie 6) is shown after restaining (Fig. 2f). The image shows the exact same focal plane where the dynamic event was observed. The newly emerged GFP^+ cell co-expresses both *c-kit* and CD31. *c-kit* staining is restricted to the newly emerged cell and to a small haematopoietic cell cluster initially present in the aorta. The pan-haematopoietic marker CD45 was not expressed by newly emerged cells (data not shown). This is not surprising since some AGM HSCs are found in the CD45⁻ fraction¹⁸. Moreover, CD45 expression is known to be delayed on HSC as compared to *c-kit* or

CD41 (refs 8, 19, 20) (CD41 discriminates the nascent cells as they commit to the haematopoietic lineage^{20,21}). Using *CD41-YFP* knock-in embryos, in which yellow fluorescent protein (YFP) expression faithfully recapitulates that of CD41 (ref. 22), we found that YFP expression begins when cells bud from the CD41⁻ endothelium (Fig. 2g and Supplementary Movie 7). The newly emerged CD41-YFP⁺ cells also co-express CD31 and *c-kit* as shown in another experiment (Supplementary Fig. 3). Hence, the emerging cells express all the markers that characterize long-term repopulating HSCs, as previously shown by *in vivo* transplantation. The inability to isolate single cells directly from a non-fixed tissue and to perform single cell transplantations with embryonic tissues precludes the functional identity of the emergent cells as HSCs at the present time. Thus, phenotypically defined HSCs (expressing *Ly-6A-GFP*, CD31, *c-kit* and CD41, but not yet CD45) emerge directly from aortic endothelial cells.

In 12 independent experiments, a total of 93 sections (with an average of 9 slices cut per embryo) were imaged. 1.7 emergent events per E10 embryo (33–36 s.p. stage) were found. This result conforms to the number of HSCs per E11 AGM (<2 HSCs) calculated by transplantation with limiting cell dilution^{23,24}. To ensure that we did not miss emergence events due to the embryo slicing technique, larger portions of the aorta were imaged using another new experimental approach (Fig. 3). After removing the somites, the whole remaining embryo was imaged with the dorsal side facing the objective of the

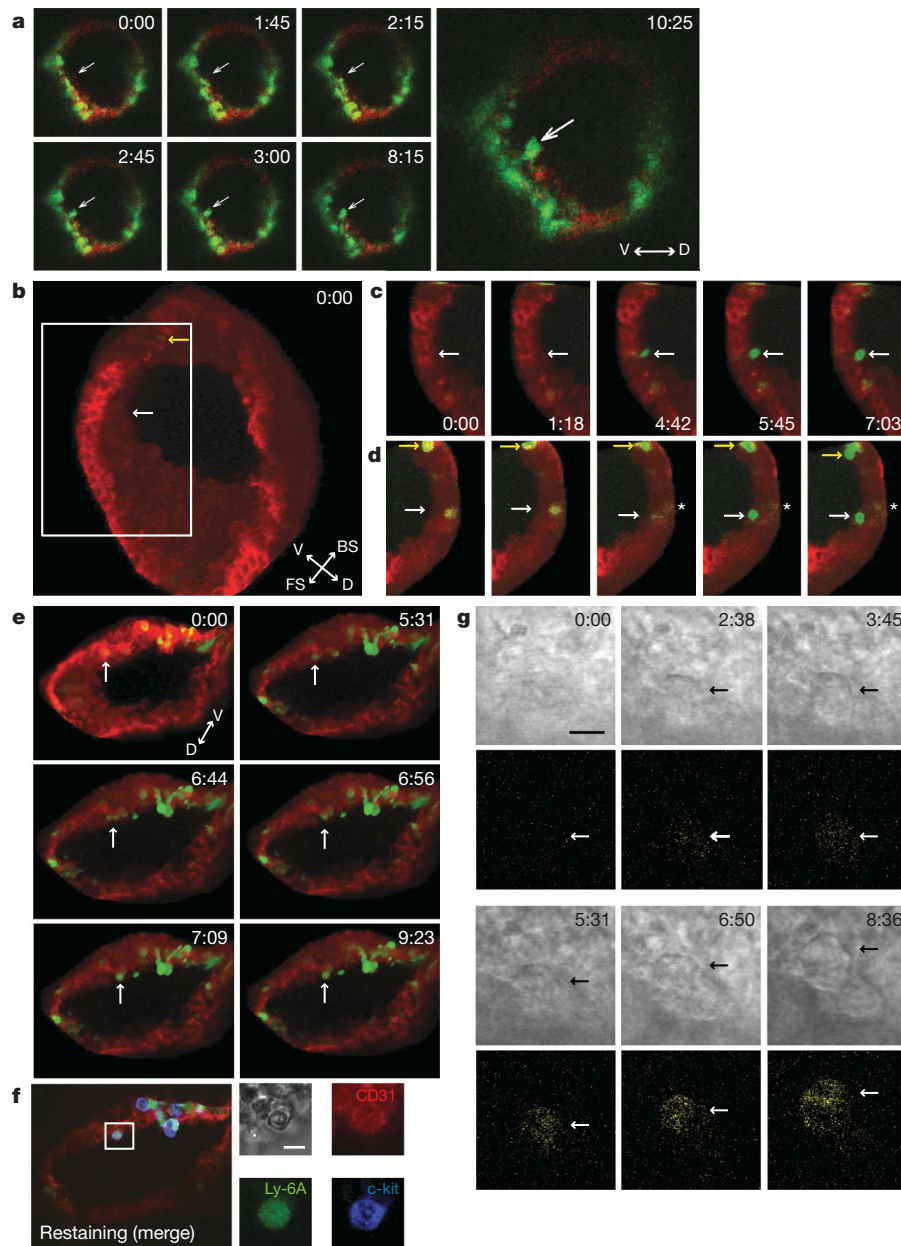


Figure 2 | Emergence of phenotypically defined HSCs on embryo slices. **a**, Time-lapse imaging of E10 *Ly-6A-GFP*⁺ embryo slice (Supplementary Movie 2). $\times 20$ lens. V, ventral side; D, dorsal side; green, *Ly-6A-GFP*; red, *CD31-PE*. **b-d**, Three-dimensional reconstruction of a time-lapse imaged aorta from an E10 *Ly-6A-GFP* embryo slice (Supplementary Movie 4). FS, front side of the aorta; BS, back side. The white box in **b** is shown in **c** (front side of the aorta) and **d** (back side). White and yellow arrows indicate the position where two cells will emerge. The asterisk in **d** points to a *GFP*⁺ cell that remains in the endothelium. $\times 40$ lens; green, *Ly-6A-GFP*; red,

CD31-Alexa 647. **e**, Time-lapse imaging of E10 *Ly-6A-GFP* embryo slice. Emergence of a *GFP*⁺ cell (arrow) (Supplementary movie 6). Green, *Ly-6A-GFP*; red, *CD31-PE*. **f**, After time-lapse imaging (**e**) the embryo slice was stained with anti-*c-kit*-allophycocyanin (APC) antibodies (blue). The boxed area (*GFP*⁺*CD31*⁺*c-kit*⁺ cell) is shown enlarged in the small right panels. **g**, Time-lapse imaging of E10 *CD41-YFP* embryo slice. Notice the cell emergence (black arrow) and the concomitant YFP expression (white arrow) (Supplementary Movie 7). Upper panel, transmitted light; lower panel, *CD41-YFP*. Scale bar, 10 μ m. Time in hours and minutes.

confocal microscope (Fig. 3a). This allows an open view, first of the aorta wall sides and second, by going deeper inside the embryo, of the aortic ventral floor (Fig. 3b). A 3D reconstruction of an aorta is shown in Fig. 3c and Supplementary Movie 8. By imaging whole E10.5 *Ly-6A-GFP* embryos overnight we again observed the emergence of *GFP*⁺ cells directly from the aortic endothelium (Fig. 3d and Supplementary Movie 9). We never observed the emergence of more than two *GFP*⁺ cells per aorta, confirming the results with embryo slices. Thus, we conclude that the emergence events in E10.5 embryo (>33 s.p.) are indeed very rare.

How haematopoietic cells emerge from the endothelium is a subject of intense interest. Two recent studies highlight the requirement of

blood flow for the induction of aortic haematopoiesis^{25,26}. The absence of blood flow during our embryo slice imaging did not impair haematopoietic cell emergence. On the basis of the results of previous AGM explant/reaggregate culture studies examining HSC development^{2,27}, the signals emanating from the circulation occur between E8.5 and early E10. Now that the dynamic emergence of haematopoietic cells can be observed directly in the live mouse embryo aorta, our approach will assist in identifying the signals necessary for each process involved in the production of these cells, such as cell morphological changes, haematopoietic commitment, and sequential surface marker modification. Our approach should also help to identify the mechanisms defective in known haematopoietic mutants.

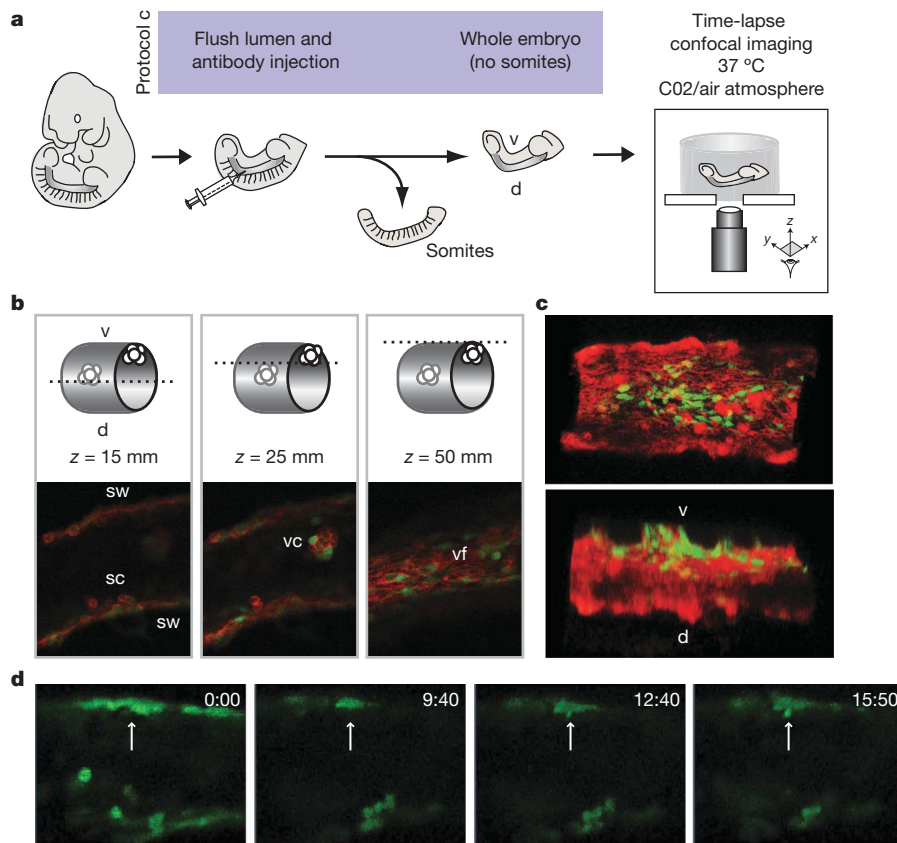


Figure 3 | Emergence of phenotypically defined HSCs in whole E10 *Ly-6A-GFP* embryos. **a**, Protocol scheme. After antibody injection in the aorta, somites were removed (protocol c). **b**, Visualization of the aortic endothelium and haematopoietic clusters in three optical planes of an aorta imaged at different depths. Upper panels: schematic representations, lower

panels: real confocal images. ao, aorta; sw, side wall; v, ventral side; d, dorsal side; vc, ventral cluster; vf, ventral floor; red, CD31–Alexa 647; green, *Ly-6A-GFP*. **c**, Three-dimensional reconstitution of the aorta. Red, CD31–Alexa 647; green, *Ly-6A-GFP* (Supplementary Movie 8). **d**, Time-lapse imaging of an aorta. Emergence of a GFP⁺ cell (arrow) (Supplementary Movie 9).

METHODS SUMMARY

Mouse embryos (E9, E10, E11) were dissected first in PBS supplemented with 10% fetal calf serum (FCS), penicillin (100 U ml^{-1}) and streptomycin ($100 \mu\text{g ml}^{-1}$) (PBS/FCS/PS) and then kept in CO_2 -independent medium with 10% FCS/PS (Gibco). Embryos were removed from the uterus and separated from placentas and all extra-embryonic membranes. The age of embryo was determined by the count of somite pairs. E9 embryos are 17–25 somite pairs (s.p.) and E10 embryos are 28–36 s.p. Head, tail and heart were removed before PBS flushing of the aorta (to eliminate all cells from the blood circulation that might attach non-specifically to the aortic endothelium) and injection of directly labelled antibodies (protocols a and c). After staining the embryo was cut into slices of $200 \mu\text{m}$ thickness by using a tissue chopper²⁸. With protocol b, antibody staining was performed after incubating embryo slices directly with the antibodies for 30 min at 4°C , followed by two washes. Protocol b allows the staining of cells also outside the aorta, in the surrounding mesenchyme (Supplementary Fig. 1). Slices were placed in a culture chamber closed at the bottom with a glass coverslip and covered with low melting point agarose gel (1%). The gel was then covered with myeloid long-term medium (STEMCELL Technologies) containing hydrocortisone (final concentration 10^{-6} M , Sigma) and recombinant murine IL-3 (BD Pharmingen)²⁴. During imaging, the culture chamber was maintained at 37°C with a heating stage and maintained in constant air with 5% CO_2 humidified atmosphere. For the live confocal imaging experiments, 7 to 11 embryos were used per experiment. An average of 6 to 8 slices per experiment was sequentially time-lapse imaged with a confocal microscope.

Full Methods and any associated references are available in the online version of the paper at www.nature.com/nature.

Received 13 October; accepted 15 December 2009.

Published online 14 February 2010.

- de Bruijn, M. F., Speck, N. A., Peeters, M. C. & Dzierzak, E. Definitive hematopoietic stem cells first develop within the major arterial regions of the mouse embryo. *EMBO J.* **19**, 2465–2474 (2000).

- Medvinsky, A. & Dzierzak, E. Definitive hematopoiesis is autonomously initiated by the AGM region. *Cell* **86**, 897–906 (1996).
- Müller, A. M., Medvinsky, A., Strouboulis, J., Grosveld, F. & Dzierzak, E. Development of hematopoietic stem cell activity in the mouse embryo. *Immunity* **1**, 291–301 (1994).
- Tavian, M. *et al.* Aorta-associated CD34⁺ hematopoietic cells in the early human embryo. *Blood* **87**, 67–72 (1996).
- Jaffredo, T., Gautier, R., Eichmann, A. & Dieterlen-Lievre, F. Intraaortic hemopoietic cells are derived from endothelial cells during ontogeny. *Development* **125**, 4575–4583 (1998).
- García-Porrero, J. A., Godin, I. E. & Dieterlen-Lievre, F. Potential intraembryonic hemogenic sites at pre-liver stages in the mouse. *Anat. Embryol. (Berl.)* **192**, 425–435 (1995).
- Dzierzak, E. & Speck, N. A. Of lineage and legacy: the development of mammalian hematopoietic stem cells. *Nature Immunol.* **9**, 129–136 (2008).
- Eilken, H. M., Nishikawa, S. & Schroeder, T. Continuous single-cell imaging of blood generation from haemogenic endothelium. *Nature* **457**, 896–900 (2009).
- Lancrin, C. *et al.* The haemangioblast generates haematopoietic cells through a haemogenic endothelium stage. *Nature* **457**, 892–895 (2009).
- Zovein, A. C. *et al.* Fate tracing reveals the endothelial origin of hematopoietic stem cells. *Cell Stem Cell* **3**, 625–636 (2008).
- Chen, M. J., Yokomizo, T., Zeigler, B. M., Dzierzak, E. & Speck, N. A. Runx1 is required for the endothelial to hematopoietic cell transition but not thereafter. *Nature* **457**, 887–891 (2009).
- Bertrand, J. Y., Kim, A. D., Teng, S. & Traver, D. CD41⁺ cmyb⁺ precursors colonize the zebrafish pronephros by a novel migration route to initiate adult hematopoiesis. *Development* **135**, 1853–1862 (2008).
- Kissa, K. *et al.* Live imaging of emerging hematopoietic stem cells and early thymus colonization. *Blood* **111**, 1147–1156 (2008).
- Ma, X., Robin, C., Ottersbach, K. & Dzierzak, E. The *Ly-6A* (*Sca-1*) *GFP* transgene is expressed in all adult mouse hematopoietic stem cells. *Stem Cells* **20**, 514–521 (2002).
- de Bruijn, M. F. *et al.* Hematopoietic stem cells localize to the endothelial cell layer in the midgestation mouse aorta. *Immunity* **16**, 673–683 (2002).
- Taoudi, S. & Medvinsky, A. Functional identification of the hematopoietic stem cell niche in the ventral domain of the embryonic dorsal aorta. *Proc. Natl Acad. Sci. USA* **104**, 9399–9403 (2007).

17. Sánchez, M. J., Holmes, A., Miles, C. & Dzierzak, E. Characterization of the first definitive hematopoietic stem cells in the AGM and liver of the mouse embryo. *Immunity* **5**, 513–525 (1996).
18. North, T. E. *et al.* Runx1 expression marks long-term repopulating hematopoietic stem cells in the midgestation mouse embryo. *Immunity* **16**, 661–672 (2002).
19. Matsubara, A. *et al.* Endomucin, a CD34-like sialomucin, marks hematopoietic stem cells throughout development. *J. Exp. Med.* **202**, 1483–1492 (2005).
20. Mikkola, H. K., Fujiwara, Y., Schlaeger, T. M., Traver, D. & Orkin, S. H. Expression of CD41 marks the initiation of definitive hematopoiesis in the mouse embryo. *Blood* **101**, 508–516 (2003).
21. Corbel, C. & Salaun, J. α IIb integrin expression during development of the murine hemopoietic system. *Dev. Biol.* **243**, 301–311 (2002).
22. Zhang, J. *et al.* CD41-YFP mice allow *in vivo* labeling of megakaryocytic cells and reveal a subset of platelets hyperreactive to thrombin stimulation. *Exp. Hematol.* **35**, 490–499 (2007).
23. Kumaravelu, P. *et al.* Quantitative developmental anatomy of definitive haematopoietic stem cells/long-term repopulating units (HSC/RUs): role of the aorta-gonad-mesonephros (AGM) region and the yolk sac in colonisation of the mouse embryonic liver. *Development* **129**, 4891–4899 (2002).
24. Robin, C. *et al.* An unexpected role for IL-3 in the embryonic development of hematopoietic stem cells. *Dev. Cell* **11**, 171–180 (2006).
25. Adamo, L. *et al.* Biomechanical forces promote embryonic haematopoiesis. *Nature* **459**, 1131–1135 (2009).
26. North, T. E. *et al.* Hematopoietic stem cell development is dependent on blood flow. *Cell* **137**, 736–748 (2009).
27. Taoudi, S. *et al.* Extensive hematopoietic stem cell generation in the AGM region via maturation of VE-cadherin⁺CD45⁺ pre-definitive HSCs. *Cell Stem Cell* **3**, 99–108 (2008).
28. Molyneaux, K. A., Stallock, J., Schaible, K. & Wylie, C. Time-lapse analysis of living mouse germ cell migration. *Dev. Biol.* **240**, 488–498 (2001).

Supplementary Information is linked to the online version of the paper at www.nature.com/nature.

Acknowledgements We thank F. Grosveld for critical discussions, T. Graf and T. Schroeder for the CD41-YFP mice and the department of Neuroscience (Erasmus MC) for the tissue chopper. This work was supported by NWO (Vidi) grant 917-76-345 (C.R., J.-C.B.), NIH R37 DK054077 (E.D.) and BSIK SCDD 03038 (E.D.).

Author Contributions C.R. and E.D. conceived ideas. C.R. designed the research. C.R. and J.-C.B. performed the experiments, analysed the data, interpreted the experiments and made the figures. C.R. and C.A.S. developed the embryo slicing technique. W.v.C. assisted with the confocal microscopy experiments. C.R., J.-C.B. and N.G. made the 3D movies. C.R. and W.v.C. made the 2D movies. C.R., J.-C.B., N.G. and E.D. wrote the manuscript. All authors discussed the results and commented on the manuscript.

Author Information Reprints and permissions information is available at www.nature.com/reprints. The authors declare no competing financial interests. Correspondence and requests for materials should be addressed to C.R. (c.robin@erasmusmc.nl).

METHODS

Embryo generation. Embryos were generated from crosses of *Ly-6A-GFP* transgenic male mice¹⁴ (heterozygous or homozygous) and wild-type (C57BL/10 × CBA)F1 females. *CD41-YFP* embryos were kindly provided by T. Schroeder and were generated from crosses of *CD41-YFP* knock-in male mice²² and wild-type (C57BL/6) females. *Runx1* embryos were generated after set up plugging between *Runx1* male and female mice (heterozygous). Genotype of *Runx1* embryos was performed by PCR as previously described²⁹. The day of vaginal plug observation is E0. Transgenic embryos were selected based on their GFP or YFP expression after microscopic observation by using an Olympus IX70 fluorescent microscope. Mice were housed according to institutional guidelines and all animal procedures were carried out in compliance with the standards for humane care and use of laboratory animals.

Antibodies and dyes. Monoclonal antibodies (BD Pharmingen, eBioscience, Invitrogen, Santa Cruz, BioLegend) used for the live imaging include: PE-anti-CD4; PE or Alexa647-anti-CD31; PE or APC-anti-c-kit; FITC, PE or APC-anti-CD45; APC-anti-CD34. The viability of embryonic slices was tested after overnight imaging. Sections were removed from the agarose gel, dissociated after collagenase digestion and cells were stained with FITC-anti-AnnexinV and 7AAD (data not shown). Analyses were performed on a FACScan. Validation of the embryo cutting and staining techniques was performed with E10 *Runx1*^{+/+} and *Runx1*^{-/-} embryo slices (Supplementary Fig. 2a). *Runx1*^{+/+} slices showed c-kit⁺CD45⁺CD31⁺ clusters attached to the CD31⁺ intra-aortic endothelium (Supplementary Fig. 2b), whereas (as expected) the slices obtained from a total of five *Runx1*^{-/-} embryos were all devoid of intra-aortic clusters and c-kit⁺ or CD45⁺ stained cells (Supplementary Fig. 2c, d)³⁰.

Multi-location time-lapse imaging. Microscopic observations were obtained by using a Zeiss LSM510 confocal microscope (Carl Zeiss), equipped with a 25 mW argon laser at 488 nm, on a heated microscope stage with a ×20 (numerical aperture (NA) 0.5) Epiplan-Neofluar dry lens or a ×40 (NA 1.2) C-Apochromat water immersion lens. GFP fluorescence was detected using a HFT488 dichroic beam splitter and an additional 505–550 bandpass emission filter placed in front of a photo multiplier tube. At the same time a transmitted light non-confocal image was made. The phycoerythrin (PE) fluorescence was detected using a 1 mW HeNe laser at 543 nm and a HFT488/543 dichroic beam splitter and an additional 565–615 bandpass emission filter. For the multicolour confocal time lapse experiments,

movies and pictures were obtained using sequential scans on a Leica SP5 confocal microscope with AOBs (Leica microsystems). YFP was excited with a 200 mW argon laser (514 nm) and measured with emission setting at 520–600 nm. GFP and FITC were excited with a 200 mW argon laser (488 nm) and measured with emission setting at 500–550 nm. PE was excited with a 10 mW DPSS laser diode (561 nm) with a 570–620 nm emission setting. Alexa 647 and APC were excited with a 10 mW HeNe (633 nm) with a 650–750 nm emission setting. Sections were imaged with a ×40 (NA 0.6) HCX-plan-fluotar lens. The microscope stage was heated to 37 °C and embryo slices were incubated with air containing 5% CO₂. Stacks of images were taken every 15 min during a period up to 15 h, in optical planes (separated by 2 to 5 μm) along a z range of 120 μm. Validation of the fluorescent staining was verified by staining embryo slices with isotype antibodies (for example, IgG2b-PE) and with anti-CD4-PE (not expressed in the aorta). No staining was observed in all cases. Moreover, in the case of multiple staining, embryos slices were stained with individual antibody to verify that no fluorescent signals were detected in the other channels (data not shown). To validate HSC emergence, all embryo slices were observed at every optical plane to verify that the emerging cell was not coming from another z-stack (up or below the z-stack of emergence).

Data analysis and image processing. After overnight time-lapse imaging, movies were made with ImageJ by compiling images from one focal plane or from the maximum projection of up to three consecutive focal planes (available at <http://rsb.info.nih.gov/ij/>). The images were aligned with the ImageJ plugin StackReg. 3D reconstitutions of aortas and time-lapse movies were processed and edited using Volocity software (Perkin Elmer) and QuickTime player (Apple). For Supplementary Movie 5, deconvolution (Huygens Deconvolution Software, Scientific Volume Imaging) with theoretical points spread function was used to increase the axial resolution and to remove noise from the images shown non deconvoluted in Fig. 2b (white arrow) and Supplementary Movie 4. One z-slice of the stack is shown in Supplementary Movie 5.

29. Cai, Z. *et al.* Haploinsufficiency of AML1 affects the temporal and spatial generation of hematopoietic stem cells in the mouse embryo. *Immunity* **13**, 423–431 (2000).
30. North, T. *et al.* *Cbfa2* is required for the formation of intra-aortic hematopoietic clusters. *Development* **126**, 2563–2575 (1999).